



## Role of specific distorted metal complexes in exciton self-trapping for hybrid metal halides†

Cite this: *Chem. Commun.*, 2020, 56, 10139

Received 10th July 2020,  
Accepted 4th August 2020

DOI: 10.1039/d0cc04778c

rsc.li/chemcomm

Romain Gautier,<sup>a</sup> Rodolphe Clérac,<sup>b</sup> Michael Paris<sup>a</sup> and Florian Massuyeau<sup>a</sup>

**A methodology enabling the discovery of hybrid metal halide phosphors through the selection of structural networks, which exhibit a specific distorted environment of the metal ions associated with the self-trapping of excitons, is proposed. This approach is demonstrated with the synthesis of an efficient near-UV emitting hybrid cadmium halide phosphor.**

Owing to the emergence of the low-dimensional hybrid perovskites as materials for optoelectronics, metal halides have recently been at the center of new attention.<sup>1,2</sup> Thus, in addition to the promising photovoltaic applications, these compounds exhibit tunable photoluminescence properties which make them interesting candidates for light emitting diode (LED) applications. Recently, the synthesis of efficient broadband emitting hybrid metal halides for solid-state lighting (SSL) has been reported.<sup>3–17</sup> Such emission is often attributed to the self-trapping of excitons (STE) as previously reported in the binary metal halides such as KX, PbX<sub>2</sub>, or CdX<sub>2</sub>, (X = halides).<sup>18</sup> In these binary materials, the STE is commonly associated with a distortion in the metal ion coordination sphere.<sup>19–22</sup> For example, in cadmium halide binary compounds, the STE was previously described as a deformation of CdX<sub>6</sub> sites which would be similar to the inherent distortion of Cu<sup>II</sup>X<sub>6</sub> moieties.<sup>23</sup> In addition, Wang *et al.* recently revealed that an STE with Jahn–Teller-like octahedral distortion would be mainly responsible of the broadband emissions observed in hybrid metal halides.<sup>22</sup> In this context, we investigated the

synthesis of cadmium and copper halides based on *trans*-2,5-dimethylpiperazine (abbreviated TDMP in the following) to unravel the relationships between ground-state distortion and STE. The present work suggests that the future discoveries of efficient hybrid metal halide phosphors could be facilitated by studying the photoluminescence properties of known materials exhibiting specific distortions.

The syntheses of the two hybrid metal halide compounds were carried out under hydrothermal conditions from mixtures of metals, HCl and *trans*-2,5-dimethylpiperazine (ESI†). A new compound based on Cd(II) isostructural to the previously reported Cu(II) compound (bond valence calculations: 1.72 v.u. and 1.85 v.u. for Cu and Cd, respectively) was isolated (Fig. S1, ESI†) and the structure was determined by single-crystal X-ray diffraction (Tables S1–S4, ESI†).<sup>24</sup> The presence of *trans*-2,5-dimethylpiperazine-1,4-dium cations (TDMP<sup>2+</sup>) was confirmed by the FTIR measurements (Fig. S2, ESI†). Elemental



Romain Gautier

Romain Gautier is currently a research scientist at Centre National de la Recherche Scientifique (CNRS) in the Institut des Matériaux Jean Rouxel. Prior to this position, he obtained a PhD degree from Ecole Nationale Supérieure de Chimie de Rennes in inorganic and materials chemistry in 2010. Then, he moved to Northwestern University as a postdoc in the group of Prof. Poeppelmeier. In 2019, he received the

CNRS Bronze medal and the National Chinese Award of “1000 Young Talents Program”. His current research interests include the design, synthesis and characterization of new inorganic and hybrid materials with properties of second harmonic generation and luminescence.

<sup>a</sup> Université de Nantes, CNRS, Institut des Matériaux Jean Rouxel, IMN, F-44000 Nantes, France. E-mail: Romain.Gautier@cnrs-imn.fr

<sup>b</sup> Univ. Bordeaux, CNRS, Centre de Recherche Paul Pascal, UMR 5031, 33600 Pessac, France

† Electronic supplementary information (ESI) available: Experimental details, Tables S1–S4, Fig. S1–S4 reporting XRD patterns, <sup>1</sup>H–<sup>113</sup>Cd and <sup>1</sup>H–<sup>15</sup>N CP-MAS NMR spectra, thermal analyses, FTIR spectra, EDX analysis, magnetic properties, temperature dependent photoluminescence, UV/Visible absorption spectra, and crystallographic information files for both compounds. CCDC 1424483 and 1424484. For ESI and crystallographic data in CIF or other electronic format see DOI: 10.1039/d0cc04778c

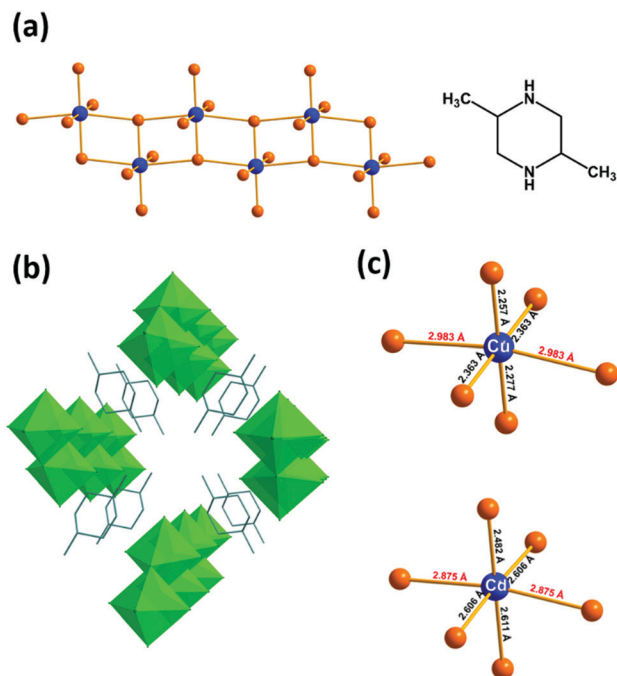


Fig. 1 Representation of (a) the ladder-type structure of copper and cadmium chloride compounds and the *trans*-2,5-dimethylpiperazine (TDMP) molecule, (b) the packing of inorganic ladders and TDMP<sup>2+</sup> cations and (c) the distortion of metal chloride octahedra.

analysis by EDS (1/4.3 for Cu/Cl and 1/4.0 for Cd/Cl) agrees with the expected M/Cl ratios (Fig. S3, ESI†). The two isostructural materials are built with anionic metal halide ladders isolated between TDMP<sup>2+</sup> cations (Fig. 1a, b and Fig. S4, ESI†). Even if these two compounds (TDMP)MCl<sub>4</sub> (M = Cu or Cd) exhibit structural similarities with the previously reported (TDMP)PbX<sub>4</sub> (X = Cl, Br, I; *i.e.* ladder structures of the metal halide, same ratio TDMP/M/X, edge-sharing MX<sub>6</sub> units, shift between adjacent ladders...),<sup>20,25</sup> some major structural differences can be observed (Fig. S5, ESI†). The structure of the latter is related to the post-perovskites: the inorganic ladder is derived from the two-dimensional post-perovskite structure by slicing perpendicularly to the *a* axis and consists of both edge-sharing and corner-sharing MX<sub>6</sub> units. On the other hand, the (TDMP)MCl<sub>4</sub> (M = Cu or Cd) structures cannot be related to the perovskite or post-perovskite structures. In the present case, the ladder is built exclusively of edge-sharing MCl<sub>6</sub> octahedral units.

The ladders in (TDMP)MCl<sub>4</sub> (M = Cu or Cd) are composed of metal chloride octahedra ( $2.2571(5) < d_{\text{Cu-Cl}} < 2.9834(1) \text{ \AA}$  for (TDMP)CuCl<sub>4</sub> and  $2.4825(7) < d_{\text{Cd-Cl}} < 2.8751(1) \text{ \AA}$  for (TDMP)CdCl<sub>4</sub>; Fig. 1c). It is important to note that a strong first-order Jahn-Teller distortion (JTD) is observed on the CuCl<sub>6</sub> octahedra motif with short and long Cu-Cl bonds perpendicular and along the ladders, respectively. More interestingly, for (TDMP)CdCl<sub>4</sub>, the cadmium also exhibits a similar distorted environment with two long Cd-Cl bonds ( $2.8751(1) \text{ \AA}$ ) along the 1D structure and four short Cd-Cl bonds ( $2.4825(7) \text{ \AA} < d_{\text{Cd-Cl}} < 2.6108(6) \text{ \AA}$ ) perpendicular to the ladder. Thus, the four chloride ligands coordinated to one or two Cd are associated

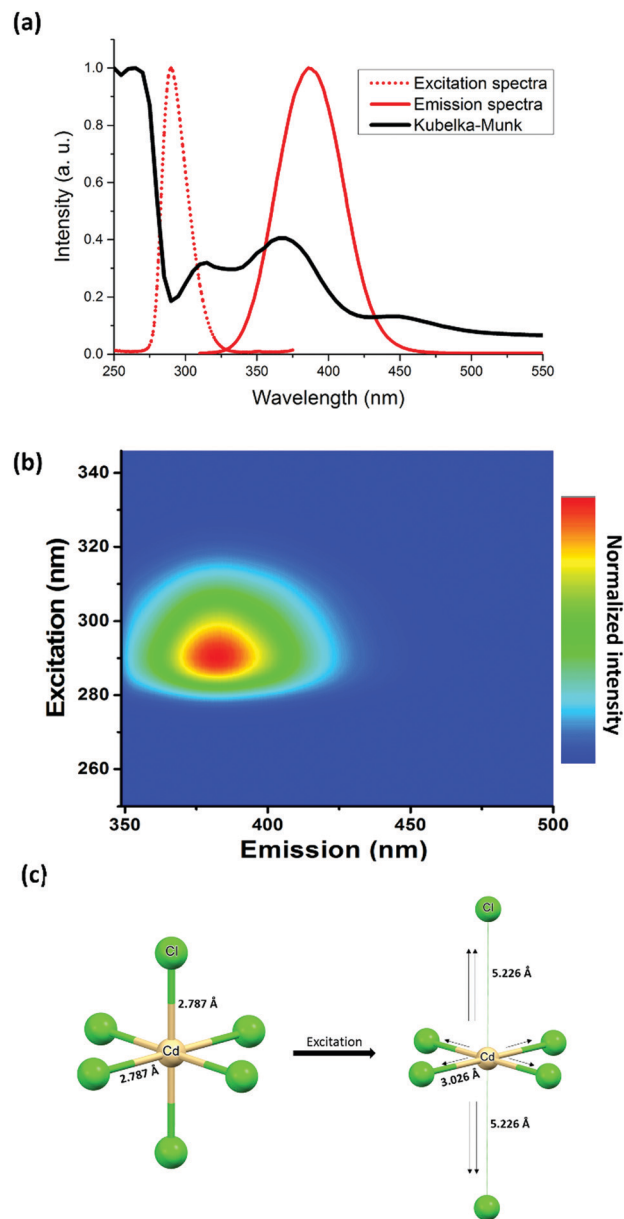


Fig. 2 (a) Absorption, excitation ( $\lambda_{\text{em}} = 385 \text{ nm}$ ), and emission ( $\lambda_{\text{exc}} = 290 \text{ nm}$ ) spectra of (TDMP)CdCl<sub>4</sub>. (b) PL excitation vs. emission mapping of (TDMP)CdCl<sub>4</sub>, and (c) calculated distortion of [CdX<sub>6</sub>]<sup>4-</sup> motifs under excitation.

with short Cd-Cl bond lengths whereas the two other ligands, in the *trans*-position to each other, are coordinated to three Cd and are associated with the longest Cd-Cl bond lengths. In addition, the distortion of the CdCl<sub>6</sub> octahedra is detected by the notable chemical shift anisotropy extracted from the spinning side bands manifold of the <sup>1</sup>H-<sup>113</sup>Cd CP-MAS NMR spectrum (Fig. S6, ESI†). The observation of such similar distortions (nearly *D*<sub>4h</sub>) for both compounds shows that the inorganic network not only accommodates such inherent *D*<sub>4h</sub> distortion of the metal complexes but is also at its origin.

Concerning the optical properties of (TDMP)CdCl<sub>4</sub>, absorption peaks observed below the bandgap at about 280 nm (Fig. 2a) can

be assigned to intra-gap states. Upon excitation at 290 nm, the  $d^{10}$  Cd(II) based compound exhibits a strong emission at 385 nm (Fig. 2a, b and Fig. S7, S8, ESI†) with a high photoluminescence quantum yield (PLQY = 40%) and a relatively high thermal stability (decomposition at about 250 °C; Fig. S9, ESI†). In addition to this intense photoluminescence (PL) emission, a weak luminescence can be observed in the visible region (around 500 nm; Fig. S10, ESI†). The observed emissions exhibit important Stokes shifts together with slight blue shifts and broadenings upon heating from 77 K to room temperature. This thermal dependence is indeed typical of emissions originating from STE. In addition, the decay times of the two emissions (0.54 ns for the high energy band and 0.69 ns for the low energy band) are similar to previously reported ones in other hybrid metal halides. Similar near-UV and green-yellow emissions are also observed for  $CdX_2$  binary compounds ( $X = Cl, Br, I$ ) at low temperature,<sup>23,26–28</sup> and these emissions were both assigned to STE associated with a distortion of the  $CdX_6$  units. To support such mechanism,<sup>23,27</sup> Nakagawa *et al.* showed that the electron paramagnetic resonance (EPR) spectra of irradiated  $CdX_2$  crystals exhibited similar structures as the ones of  $Cu^{2+}$  or  $Ag^{2+}$  doped cadmium halide crystals. Thus, this observation suggested that the excited states of the  $CdX_6$  units would be symmetrically similar to the inherent distortion of the  $Cu^{2+}$  based octahedral complex.

To further unravel the deformation of the inorganic lattice responsible for the STE, DFT and TDDFT calculations were carried out (see details in the ESI†). After optimizing the excited state of  $[CdX_6]^{4-}$  units, a deformation corresponding to a  $D_{4h}$  distortion (lengthening of two opposite Cd–X bonds associated with the shortening of four equatorial Cd–X bonds) was observed (Fig. 2c). Interestingly, another recent theoretical investigation of the 0D lead perovskite,  $Cs_4PbBr_6$ , suggested that the STE occurs with the same distortion: shortening of four Pb–Br equatorial bonds together with the elongation of the two remaining bonds.<sup>29</sup> The calculation of the electronic DOS of the STE structure showed the presence inside the band gap of an unoccupied hole state (Br p + Pb s) with an occupied electron state (Pb p + Br p). In addition, the same chains have been reported for the broad-band emitters  $C_4N_2H_{14}PbX_4$  ( $X = Cl, Br$ ,  $C_4N_2H_{14} = N,N'$ -dimethylethylene-1,2-diammonium),<sup>30,31</sup> exhibiting relatively high photoluminescence quantum yields (PLQYs about 20%). Concerning the chloride analogue, Wu *et al.* proposed that the emission originates from the distortion of the six Pb–X bonds with a contraction of four planar Pb–X bonds and elongation of the two other Pb–X bonds. Following this work, Wang *et al.* performed DFT calculations on the lead bromide ladder-like chains.<sup>31</sup> They identified two STEs, one Jahn–Teller like (STE1) at high energy which is the most stable and one non-Jahn–Teller at lower energy (STE2). Thus, the two emissions at 385 and 500 nm for our cadmium chloride, could be related to the same mechanisms. Interestingly, the STE through a Jahn–Teller like distortion has also been reported for other metal halides such as  $Cs_2AgInCl_6$  in which  $AgCl_6$  distortion was shown to be responsible for highly efficient broad-band emission. Thus, this Jahn–Teller distortion could be a general phenomenon which occurs in the excited states and would be at the origin of the broadband luminescence of many metal halides.

In  $(TDMP)CdCl_4$ , the  $D_{4h}$  distortion of the  $CdX_6$  units induced by the inorganic network is already observed in the ground state. Such distortion would also promote the STE and the enhancement of the associated luminescence. Thus, the intra-gap states observed in the absorption spectra (Fig. 2a) would be associated with the distorted  $CdX_6$  units, which would behave as traps for the excitons (extrinsic self-trapping). Promoting this distortion by targeting crystal structures in which the excited states are likely to form could also be an interesting strategy to synthesize materials with enhanced photoluminescence from STE. Of particular interest, families of isostructural metal (Cu(II), Cd(II) and Pb(II)) halide materials would be interesting to explore. If the inherent Jahn–Teller distortion of the Cu(II) site is possible in a specific network, one can expect the same distortion to be possible in the excited states when considering other metal ions such as Cd(II) and Pb(II).

In addition to the specific distortion of the  $MX_6$  octahedral units, other structural features help to assist the STE and prevent the PL quenching. Thus, similar to previously reported lead halide ladders, lowering the dimensionality lowers the deformation energy and the associated barrier to self-trapping.<sup>18,25</sup> This phenomenon would explain why intense STE emissions can be observed at room temperature for the 0D and 1D metal halides whereas the 2D or 3D systems such as the binary  $MX_2$  show intense STE emission only at cryogenic temperatures. To prevent PL quenching, the organic cations should also hardly interact with the inorganic metal halide.<sup>20</sup> In the  $(TDMP)CdCl_4$ , the organic cations are favorably far from the inorganic ladders. To evaluate the organic–inorganic interactions, one can compare the bond distances of the organic molecules in the hybrid structure vs. the halide salt.<sup>20</sup> In  $(TDMP)Cl_2$ ,<sup>32</sup> the C–C and C–N bond distances are very similar to the one in  $(TDMP)CdCl_4$  (Table S2, ESI†).  $^{13}C$  NMR spectroscopy is another way to check the organic–inorganic interactions. Fig. 3 shows the  $^1H$ – $^{13}C$  CP-MAS NMR spectrum of  $(TDMP)CdCl_4$ . Although a single crystallographic site was determined by X-ray diffraction, the resonances of  $CH_3$  (15–18 ppm),  $CH_2$  (47–50 ppm) and  $CH$  (50–53 ppm) moieties exhibit multiple lines. It is likely that the resonance splits originate from the hydrogen bond network between the organic and inorganic parts of the compound. As already described, the inorganic chains of the

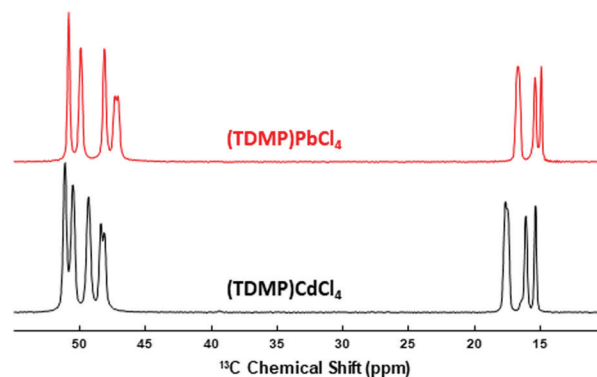


Fig. 3  $^1H$ – $^{13}C$  CP-MAS NMR spectra of  $(TDMP)CdCl_4$  and  $(TDMP)PbCl_4$ .



(TDMP)CdCl<sub>4</sub> and (TDMP)PbCl<sub>4</sub> materials differ. However, the local environment of the TDMP<sup>2+</sup> cations is highly similar within these two structures (Fig. S11, ESI†). This strong similarity, including the hydrogen bond network, is supported by the strong resemblance between the <sup>1</sup>H–<sup>13</sup>C CP-MAS NMR spectrum of (TDMP)CdCl<sub>4</sub> and those of (TDMP)PbCl<sub>4</sub> (Fig. 3) and its bromide counterpart (TDMP)PbBr<sub>4</sub> previously reported.<sup>33</sup> Moreover, for this latter material, we showed that the interactions between the organic and inorganic parts are weak.<sup>20</sup> Hence, weak interactions between the TDMP<sup>2+</sup> cations and cadmium chloride ladders would prevent the PL quenching by the C–H vibration modes.<sup>20,34,35</sup>

In summary, a new type of cadmium halide ladder-like chain with intense photoluminescence was isolated. The one-dimensional structure as well as photoemission originating from the STE show similarities with previously reported post-perovskite related lead halide compounds. The analysis of the crystal structures and associated properties shows that the STE can be assisted by specific distortions around the metal ion. In the case of (TDMP)CdCl<sub>4</sub>, the excited states would be related to the distortion of the CdCl<sub>6</sub> octahedral motif, which is similar to the inherent first-order Jahn–Teller distortion of Cu<sup>II</sup>Cl<sub>6</sub> units. Such distortion can be well accommodated in this ladder-type structure as shown by the isostructural (TDMP)CuCl<sub>4</sub> that could also be prepared using the same experimental conditions. As a multitude of Cu(II) halide phases with Jahn–Teller distortion have been synthesized and thoroughly investigated in the past for their magnetic properties, a future methodology could consist of synthesizing isostructural metal (Cd(II), Pb(II)...) halides in order to directly target materials in which the STE and the associated photoluminescence would be promoted. A first approach could consist of identifying, through the use of structural databases such as the Cambridge Structural Database (CSD), previously reported hybrid metal halides (particularly Cd(II) and Pb(II) based systems) isostructural to hybrid copper(II) halides and investigate their photoluminescence properties. Such strategy could greatly accelerate the discovery of phosphors with high photoluminescence quantum yields for LED applications.

This work was supported by the CNRS, the National Agency for Research (ANR Young Researchers, ANR-16-CE08-0003-01, Combi-SSL project), the Region Pays de la Loire (Etoiles montantes en Pays de la Loire 2017, project “Découverte de pérovskites hybrides assistée par ordinateur”), the University of Bordeaux, the Région Nouvelle Aquitaine, the MOLSPIN COST action CA15128, and the GdR MCM-2. Calculations were conducted at Centre de Calcul Intensif des Pays de la Loire, Université de Nantes. We thank Stéphane Grolleau for thermal measurements on both materials.

## Conflicts of interest

There are no conflicts to declare.

## References

- 1 M. I. Saidaminov, O. F. Mohammed and O. M. Bakr, *ACS Energy Lett.*, 2017, **2**, 889–896.
- 2 B. Saparov and D. B. Mitzi, *Chem. Rev.*, 2016, **116**, 4558–4596.
- 3 A. Nagami, K. Okamura and T. Ishihara, *Phys. B*, 1996, **227**, 346–348.
- 4 T. Ishihara, *Optical Properties of Low-dimensional Materials*, World Scientific, 1996, pp. 288–339.
- 5 E. R. Dohner, E. T. Hoke and H. I. Karunadasa, *J. Am. Chem. Soc.*, 2014, **136**, 1718–1721.
- 6 L. Mao, Y. Wu, C. C. Stoumpos, M. R. Wasielewski and M. G. Kanatzidis, *J. Am. Chem. Soc.*, 2017, **139**, 5210–5215.
- 7 L. Mao, P. Guo, M. Kepenekian, I. Hadar, C. Katan, J. Even, R. D. Schaller, C. C. Stoumpos and M. G. Kanatzidis, *J. Am. Chem. Soc.*, 2018, **140**, 13078–13088.
- 8 R. Rocanova, M. Houck, A. Yangui, D. Han, H. Shi, Y. Wu, D. T. Glatzhofer, D. R. Powell, S. Chen, H. Fourati, A. Lussan, K. Boukheddaden, M.-H. Du and B. Saparov, *ACS Omega*, 2018, **3**, 18791–18802.
- 9 A. Yangui, R. Rocanova, T. M. McWhorter, Y. Wu, M.-H. Du and B. Saparov, *Chem. Mater.*, 2019, **31**, 2983–2991.
- 10 C. Zhou, H. Lin, Y. Tian, Z. Yuan, R. Clark, B. Chen, L. J. van de Burgt, J. C. Wang, Y. Zhou, K. Hanson, Q. J. Meisner, J. Neu, T. Besara, T. Siegrist, E. Lambers, P. Djurovich and B. Ma, *Chem. Sci.*, 2018, **9**, 586–593.
- 11 Y.-Y. Guo, J. A. McNulty, N. A. Mica, I. D. W. Samuel, A. M. Z. Slawin, M. Bühl and P. Lightfoot, *Chem. Commun.*, 2019, **55**, 9935–9938.
- 12 G. Zhou, X. Jiang, M. Molokeev, Z. Lin, J. Zhao, J. Wang and Z. Xia, *Chem. Mater.*, 2019, **31**, 5788–5795.
- 13 Z. Song, J. Zhao and Q. Liu, *Inorg. Chem. Front.*, 2019, **6**, 2969–3011.
- 14 R. Zhang, X. Mao, Y. Yang, S. Yang, W. Zhao, T. Wumaier, D. Wei, W. Deng and K. Han, *Angew. Chem., Int. Ed.*, 2019, **58**, 2725–2729.
- 15 G. Zhou, B. Su, J. Huang, Q. Zhang and Z. Xia, *Mater. Sci. Eng., R*, 2020, **141**, 100548.
- 16 G. Song, M. Li, Y. Yang, F. Liang, Q. Huang, X. Liu, P. Gong, Z. Xia and Z. Lin, *J. Phys. Chem. Lett.*, 2020, **11**, 1808–1813.
- 17 C. Deng, G. Zhou, D. Chen, J. Zhao, Y. Wang and Q. Liu, *J. Phys. Chem. Lett.*, 2020, **11**, 2934–2940.
- 18 K. S. Song and R. T. Williams, *Self-Trapped Excitons*, Springer-Verlag, Berlin Heidelberg, 1993.
- 19 J. Luo, X. Wang, S. Li, J. Liu, Y. Guo, G. Niu, L. Yao, Y. Fu, L. Gao, Q. Dong, C. Zhao, M. Leng, F. Ma, W. Liang, L. Wang, S. Jin, J. Han, L. Zhang, J. Etheridge, J. Wang, Y. Yan, E. H. Sargent and J. Tang, *Nature*, 2018, **563**, 541–545.
- 20 R. Gautier, F. Massuyeau, G. Galnon and M. Paris, *Adv. Mater.*, 2019, **31**, 1807383.
- 21 M.-H. Tremblay, F. Thouin, J. Leisen, J. Bacsá, A. R. Srimath Kandada, J. M. Hoffman, M. G. Kanatzidis, A. D. Mohite, C. Silva, S. Barlow and S. R. Marder, *J. Am. Chem. Soc.*, 2019, **141**, 4521–4525.
- 22 X. Wang, W. Meng, W. Liao, J. Wang, R.-G. Xiong and Y. Yan, *J. Phys. Chem. Lett.*, 2019, **10**, 501–506.
- 23 M. Kitaura, H. Nakagawa, K. Fukui, M. Fujita, T. Miyanaga and M. Watanabe, *J. Electron Spectrosc. Relat. Phenom.*, 1996, **79**, 175–178.
- 24 Ü. Kersen, A. Wojtczak, A. Bienko and J. Jezierska, *New J. Chem.*, 2018, **42**, 15705–15713.
- 25 R. Gautier, M. Paris and F. Massuyeau, *J. Am. Chem. Soc.*, 2019, **141**, 12619–12623.
- 26 M. Kitaura and H. Nakagawa, *J. Lumin.*, 1995, **66–67**, 438–442.
- 27 H. Nakagawa and M. Kitaura, *International Conference on Excitonic Processes in Condensed Matter*, International Society for Optics and Photonics, 1995, vol. 2362, pp. 294–304.
- 28 S. Kawabata and H. Nakagawa, *J. Lumin.*, 2007, **126**, 48–52.
- 29 B. Kang and K. Biswas, *J. Phys. Chem. Lett.*, 2018, **9**, 830–836.
- 30 Z. Yuan, C. Zhou, Y. Tian, Y. Shu, J. Messier, J. C. Wang, L. J. van de Burgt, K. Kountouriotis, Y. Xin, E. Holt, K. Schanze, R. Clark, T. Siegrist and B. Ma, *Nat. Commun.*, 2017, **8**, 14051.
- 31 G. Wu, C. Zhou, W. Ming, D. Han, S. Chen, D. Yang, T. Besara, J. Neu, T. Siegrist, M.-H. Du, B. Ma and A. Dong, *ACS Energy Lett.*, 2018, **3**, 1443–1449.
- 32 J. C. J. Bart, I. W. Bassi and R. Scordamaglia, *Acta Crystallogr., Sect. B: Struct. Crystallogr. Cryst. Chem.*, 1978, **34**, 2760–2764.
- 33 H. Yuan, F. Massuyeau, N. Gautier, A. B. Kama, E. Faulques, F. Chen, Q. Shen, L. Zhang, M. Paris and R. Gautier, *Angew. Chem.*, 2020, **132**, 2824–2829.
- 34 D. Cortecchia, J. Yin, A. Bruno, S.-Z. A. Lo, G. G. Gurzadyan, S. Mhaisalkar, J.-L. Brédas and C. Soci, *J. Mater. Chem. C*, 2017, **5**, 2771–2780.
- 35 A. Yangui, D. Garrot, J. S. Lauret, A. Lussan, G. Bouchez, E. Deleporte, S. Pillet, E. E. Bendeif, M. Castro, S. Triki, Y. Abid and K. Boukheddaden, *J. Phys. Chem. C*, 2015, **119**, 23638–23647.